

Article

Intermolecular Proton Transfer in Anionic Complexes of Uracil with Alcohols

Maciej Haraczyk, Janusz Rak, Maciej Gutowski, Dunja Radisic, Sarah T. Stokes, and Kit H. Bowen

J. Phys. Chem. B, **2005**, 109 (27), 13383-13391 • DOI: 10.1021/jp050246w • Publication Date (Web): 16 June 2005

Downloaded from <http://pubs.acs.org> on May 6, 2009

More About This Article

Additional resources and features associated with this article are available within the HTML version:

- Supporting Information
- Links to the 11 articles that cite this article, as of the time of this article download
- Access to high resolution figures
- Links to articles and content related to this article
- Copyright permission to reproduce figures and/or text from this article

[View the Full Text HTML](#)



ACS Publications
High quality. High impact.

Intermolecular Proton Transfer in Anionic Complexes of Uracil with Alcohols

Maciej Harańczyk,^{†,‡} Janusz Rak,[†] and Maciej Gutowski^{*,†,‡}

Department of Chemistry, University of Gdańsk, Sobieskiego 18, 80-952 Gdańsk, Poland, and Chemical Sciences Division, Pacific Northwest National Laboratory, Richland, Washington 99352

Dunja Radisic, Sarah T. Stokes, and Kit H. Bowen, Jr.*

Department of Chemistry, Johns Hopkins University, Baltimore, Maryland 21218

Received: January 14, 2005; In Final Form: April 25, 2005

A series of 18 alcohols (ROH) has been designed with an enthalpy of deprotonation in the gas phase (H_{DP}) in the range 13.8–16.3 eV. The effects of excess electron attachment to the binary alcohol–uracil (ROH \cdots U) complexes have been studied at the density functional level with a B3LYP exchange–correlation functional and at the second-order Møller–Plesset perturbation theory level. The photoelectron spectra of anionic complexes of uracil with 3 alcohols (ethanol, 2,2,3,3,3-pentafluoropropanol, and 1,1,1,3,3,3-hexafluoro-2-propanol) have been measured with 2.54 eV photons. For ROHs with deprotonation enthalpies larger than 14.8 eV, only the ROH \cdots U $^-$ minimum exists on the potential energy surface of the anionic complex. For alcohols with deprotonation enthalpies in the range 14.3–14.8 eV, two minima might exist on the anionic potential energy surface, which correspond to the RO $^-$ \cdots HU \cdot and ROH \cdots U $^-$ structures. For ROHs with deprotonation enthalpies smaller than 14.3 eV, the excess electron attachment to the ROH \cdots U complex always induces a barrier-free proton transfer from the hydroxyl group of ROH to the O8 atom of U, with the product being RO $^-$ \cdots HU \cdot .

I. Introduction

Low-energy electrons are important for radiation-induced chemical reactions.^{1–3} A variety of negatively charged clusters involving biologically important molecules have been extensively studied, both experimentally⁴ and theoretically.^{5–13} Anions of nucleic acid bases (NAB) solvated by water and by rare gases have been studied using anion photoelectron spectroscopy^{14–16} and Rydberg electron-transfer spectroscopy.^{4,17,18}

The issue of anionic states of NABs proved to be difficult to resolve using conventional highly correlated electronic structure methods because of the size of the systems.^{5–9,13,19–24} The existence of dipole-bound states of NABs has been predicted theoretically⁵ and confirmed experimentally.^{14,17} The canonical tautomer of uracil (U), for example, supports a dipole-bound anionic state with a measured electron vertical detachment energy (VDE) of 0.093 ± 0.007 ¹⁴ and 0.085 ± 0.015 ¹⁸ eV and a calculated value of 0.073 eV.²⁴ Aflatooni et al. characterized temporary anionic states of NABs in electron transmission spectroscopy experiments and reported an electron vertical attachment energy of -0.22 eV for uracil.²⁵ It means that the anionic state of uracil at the equilibrium geometry of the neutral molecule is temporary (i.e., unstable against electron auto-detachment) and makes its appearance as a “resonance” peak in electron-scattering cross-sections. These experiments, however, do not provide information about the electronic stability of anionic states at the equilibrium geometry of the anion. Our recent CCSD(T) results indicate that the valence anionic state of the canonical tautomer of U is vertically stable with respect

to the neutral by 0.506 eV.²⁴ However, the valence anionic state is unstable, in terms of electronic energy corrected for zero-point vibrations, by 0.122 eV with respect to the dipole-bound state.²⁴ The current view is that valence anionic states of the canonical NABs are unbound or weakly bound in the gas phase, but become dominant for solvated species.^{13,20–24} However, these tautomers that result from enamine–imine transformations might be adiabatically bound with respect to the neutral species.^{23,24}

The intra- and intermolecular tautomerizations involving NABs have long been suggested as critical steps in mutations of the DNA genetic material.^{26–28} The intramolecular proton-transfer reactions have been studied for isolated and hydrated NABs.^{4,28–31} The intermolecular single and double proton-transfer reactions have been studied for the dimers of NABs and their simplified molecular models in ground and excited electronic states.^{32–36,37} It has recently been suggested that hydrogenated nucleic acid bases, which might result from intermolecular proton transfer to the anionic NAB, could play a role in the damage of DNA and RNA.³⁸ These radicals were suggested as intermediates in the processes of single strand breaks of DNA with very small barriers.

In our previous studies, we described an intermolecular proton-transfer induced by an excess electron attachment to the complex of a pyrimidine NAB with a weak acid (HA). The electron attachment might lead to a barrier-free proton transfer (BFPT) from the weak acid to the O8 atom of uracil or thymine (see Figure 1 for the numbering of atoms)^{39–41} with the products being a neutral radical of hydrogenated NAB (NAB + H \cdot) and an anion of the deprotonated acid (A $^-$)



* maciej.gutowski@pnl.gov; kbowen@jhu.edu.

[†] University of Gdańsk.

[‡] Pacific Northwest National Laboratory.

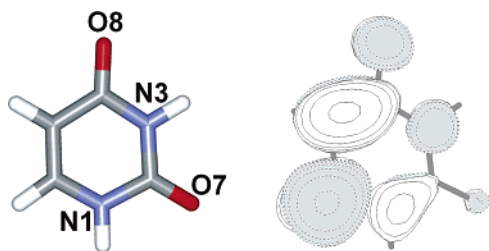


Figure 1. Labeling of atoms for uracil and excess electron distribution in valence anionic state of uracil.

The driving force for proton transfer is the stabilization of the excess electron onto the π^* orbital of the base (see Figure 1). The findings related to BFPT were based on the anion photoelectron spectroscopy (PES) measurements and the results of quantum chemical calculations.

In our previous studies, we investigated anionic complexes of a uracil or thymine with a specific proton donor, HA.^{39–41} The results of these studies suggested that the occurrence of BFPT is an outcome of interplay between the deprotonation energy of the proton donor HA, the protonation energy of the anion of NAB, and the hydrogen bonding effects. However, a limited set of HAs did not allow us to monitor a transition from the complexes without intermolecular proton transfer, that is, $\text{NAB}^- \cdots \text{HA}$, to the $(\text{NAB} + \text{H}) \cdots \text{A}^-$ complexes.

The goal of this study is to characterize binary anionic complexes formed between uracil and alcohols of different gas-phase acidity. We designed a series of 18 alcohols (ROH) with gas-phase deprotonation enthalpies (H_{DP}) in the range 13.8–16.3 eV. This range covers the region that is relevant for proton transfer in anionic complexes of uracil with ROHs. The neutral and anionic complexes have been studied at the density functional theory level with a B3LYP exchange–correlation functional and at the second-order Møller–Plesset perturbation theory level. The photoelectron spectra of the anionic complexes of uracil with 3 alcohols (ethanol, 2,2,3,3,3-pentafluoropropanol, and 1,1,1,3,3,3-hexafluoro-2-propanol) have been measured with 2.54 eV photons. The evolution of the structure of the anionic complexes of uracil with ROHs has been determined as a function of the gas-phase acidity of ROH. The reported PES spectra of 3 anionic uracil–alcohol complexes are in good agreement with the theoretical predictions.

II. Methods

II.1. Experimental methods. Negative-ion photoelectron spectroscopy is conducted by crossing a mass-selected beam of negative ions with a fixed-frequency laser beam and energy-analyzing the resultant photodetached electrons.⁴² It is governed by the energy-conserving relationship $h\nu = \text{EBE} + \text{EKE}$, where $h\nu$ is the photon energy, EBE is the electron binding energy, and EKE is the electron kinetic energy. One knows the photon energy of the experiment, one measures the electron kinetic energy spectrum, and then by difference, one obtains electron binding energies, which in effect are the transition energies from the anion to the various energetically accessible states of its corresponding neutral.

Our apparatus has been described elsewhere.⁴³ To prepare the species of interest, uracil was placed in the stagnation chamber of a nozzle source and heated to ~ 180 °C. The expansion gas was a 5% alcohol/argon mixture. Its total pressure was 1–2 atm, and the nozzle diameter was 25 μm . Electrons were injected into the emerging jet expansion from a biased Th/Ir filament in the presence of an axial magnetic field. The resulting anions were extracted and mass-selected with a

magnetic sector mass spectrometer. Electrons were then photo-detached from the selected anions with ~ 100 circulating watts of 2.540 eV photons and finally energy-analyzed with a hemispherical electron energy analyzer with a resolution of 25 meV.

Since there was very little heating of the source involved in these experiments and since the expansion occurred in a large volume of argon, we expect that both the neutrals and eventually the anions were quite cool, and thus, the complexes were in low-energy configurations.

II.2. Computational Methods. As in our earlier studies,^{39,40} we applied the density functional theory (DFT) method with a hybrid B3LYP functional^{44–46} and the 6-31++G** basis set.^{47,48} Five d functions were used on heavy atoms. We have tested that this basis set provides the B3LYP values of VDEs and stabilization energies in anionic complexes, which are converged to 0.03 eV with respect to the basis set saturated limits. The calculations of matrices of second derivatives of energy (Hessians) were performed to confirm that final geometries were minima or transition states on potential energy surfaces.

The usefulness of the B3LYP/6-31++G** method to describe intra- and intermolecular hydrogen bonds has been demonstrated in recent studies through comparison with the second-order Møller–Plesset (MP2) predictions.^{49–52} The ability of the B3LYP method to predict excess electron binding energies has recently been reviewed, and the results were found to be satisfactory for valence-type molecular anions.⁵³ We found that the value of electron VDE determined at the B3LYP/6-31++G** level for the valence π^* anionic state of an isolated uracil is overestimated by 0.2 eV in comparison with the CCSD(T)/aug-cc-pVDZ result.^{24,39} We will assume in the following that the same shift of -0.2 eV applies to the values of VDE for all anionic uracil–alcohol complexes, in which an excess electron occupies a π^* orbital localized on uracil. We also found that the VDE of the isolated uracil anion calculated at the MP2/6-31++G** (5d) level of theory is underestimated by 0.1 eV in comparison with the CCSD(T)/aug-cc-pVDZ value, and we will assume that the same shift of $+0.1$ eV applies to all anionic uracil–alcohol complexes. These corrections to the B3LYP/6-31++G** and MP2/6-31++G** levels turned out to be very effective in predicting the PES spectra of anionic complexes of NABs.^{39–41}

Sevilla et al. addressed a problem²¹ regarding which set of atomic orbitals should be used in calculations of valence anions of polar molecules, such as uracil, which are characterized by negative values of vertical electron affinity, that is, the valence anion is unbound with respect to the neutral at the optimal geometry of the neutral, but which support dipole-bound anionic states. There is a dilemma regarding what kind of the basis set should be used in calculations for the valence anionic state. On one hand, it is known that extended basis sets supplemented with basis functions with small exponents are required to properly describe diffuse charge distributions of molecular anions.⁵⁴ On the other hand, optimization of the wave function for an unbound anion of a polar molecule might converge to a solution which is contaminated with a dipole-bound contribution, if an extended basis set is used. Fortunately, the systems studied by us here are characterized by values of VDE larger than 1.1 eV, whereas typical values of electron binding energies for nucleic acid bases in dipole-bound states do not exceed 0.1 eV.^{5,8,9,22,24} Thus, our calculations can be performed with standard basis sets that contain basis functions with small exponents. Because we are dealing with bound anionic states,

TABLE 1: B3LYP/6-31++G (5d) Values of Gas-Phase Acidity Measured by Deprotonation Energy, Enthalpy, and Free Energy for Selected ROH Molecules and Hydrogenated Uracil**

symbol	molecule	gas-phase acidity				
		E_{DP}	H_{DP}	G_{DP}	H_{DP}^{exp}	G_{DP}^{exp}
A0	H ₂ O	17.155	16.859	16.555	16.937 ± 0.004 ^a	16.651 ± 0.009 ^a
A1	CH ₃ CH ₂ OH	16.656	16.277	15.949	16.401 ± 0.044 ^b	16.111 ± 0.048 ^b
A2	CH ₂ FCH ₂ OH	16.235	15.873	15.551	16.090 ± 0.125 ^c	15.800 ± 0.124 ^c
A3	CHF ₂ CH ₂ OH	16.012	15.654	15.337	15.883 ± 0.095 ^d	15.572 ± 0.087 ^d
A4	CF ₃ CH ₂ OH	15.781	15.425	15.112	15.676 ± 0.104 ^d	15.355 ± 0.087 ^d
A5	CF ₃ CF ₂ CF ₂ CH ₂ OH	15.720	15.352	15.001	15.178 ± 0.279 ^e	14.888 ± 0.259 ^e
A6	CF ₃ CF ₂ CH ₂ OH	15.660	15.302	15.002	15.406 ± 0.269 ^e	15.116 ± 0.259 ^e
A7	CCl ₃ CH ₂ OH	15.461	15.135	14.762		
A8	CH ₂ FCHFOH	15.306	14.964	14.611		
A9	CH ₂ ClCHFOH	15.166	14.828	14.472		
A10t	(CF ₃) ₂ CHOH- <i>trans</i>	15.112	14.765	14.415	14.951 ± 0.091 ^f	14.671 ± 0.087 ^f
A10c	(CF ₃) ₂ CHOH- <i>cis</i>	15.061	14.719	14.365	14.951 ± 0.091 ^f	14.671 ± 0.087 ^f
A10c	(CF ₃) ₂ CHOH- <i>cis</i> (CH) ^g	15.698	15.346	14.979	14.951 ± 0.091 ^f	14.671 ± 0.087 ^f
A11	CHF ₂ CHFOH	15.009	14.672	14.316		
A12	CF ₃ CHFOH	14.799	14.464	14.115		
A13	CClF ₂ CHFOH	14.710	14.379	14.025		
A14	CCl ₂ FCHFOH	14.708	14.375	14.016		
A15	CCl ₃ CHFOH	14.651	14.319	13.958		
A16	CH ₂ FCF ₂ OH	14.641	14.323	13.968		
A17	CHF ₂ CF ₂ OH	14.333	14.019	13.672		
A18	CF ₃ CF ₂ OH	14.097	13.785	13.444		
	HU· C5 side	14.697	14.410	14.098		
	HU· N3 side	14.650	14.367	14.034		

^a ref 65. ^b ref 66. ^c ref 67. ^d ref 68. ^e ref 69. ^f ref 70. ^g The H atom connected to C2 of A10c is important in the aA10cU complexes. See section IV.

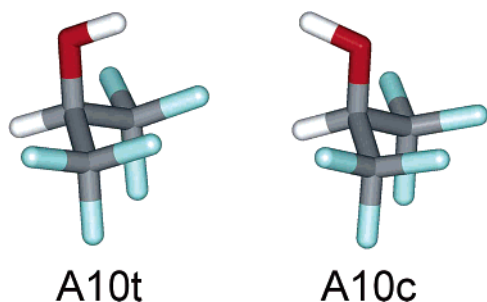
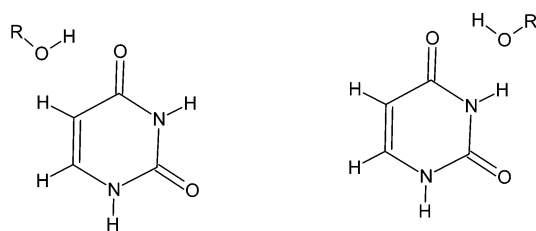


Figure 2. Two important isomers of 1,1,1,3,3,3-hexafluoro-2-propanol (A10).



C side bonding (aAnUC)

N side bonding (aAnUN)

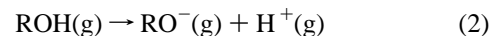
Figure 3. Two families of uracil–alcohol complexes considered in this study. The first hydrogen bond is between O8 of uracil and the hydroxyl group of ROH. The second hydrogen bond involves either N3H or C5H of uracil. These two families are denoted aAnUN and aAnUC, respectively.

these basis functions might contribute to the proper description of the anionic charge distribution but do not lead to a collapse to a dipole-bound state, which is usually less strongly bound than the valence anionic state.^{22,24}

Electronically unbound anionic states are much more difficult for theoretical characterization when using conventional electronic structure methods than electronically bound anionic states. Special treatments, such as stabilization method or complex coordinate technique, provide a more formal means to extract

resonance positions and widths.^{54,55} Alternatively, energies obtained in B3LYP calculations might provide estimates of vertical electron attachment energies.^{56,57}

The gas-phase acidity of an alcohol ROH is associated with the values of deprotonation energy (E_{DP}), enthalpy (H_{DP}), and free energy (G_{DP}). They are defined as the change of the corresponding thermodynamic function for the reaction



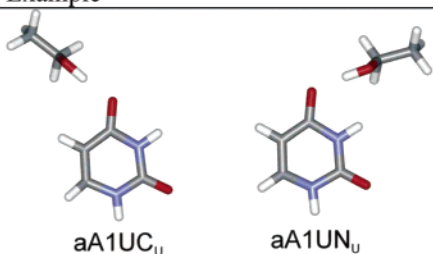
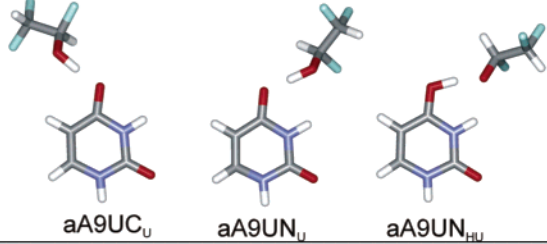
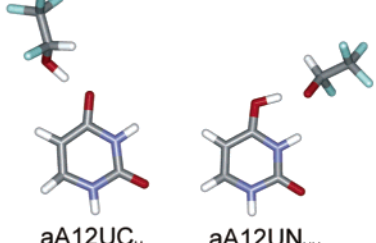
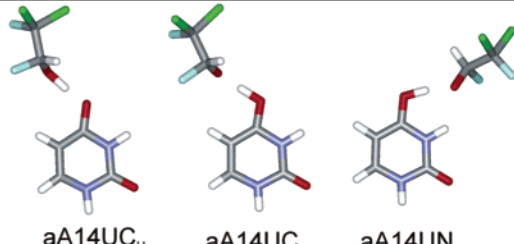
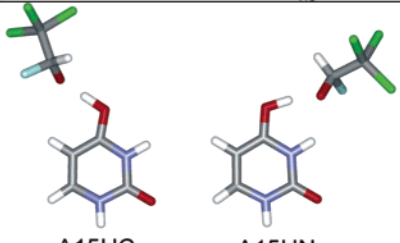
The values of H_{DP} and G_{DP} were calculated in the harmonic oscillator–rigid rotor approximation for $T = 298$ K and $p = 1$ atm. The smaller the value of E_{DP} (H_{DP} or G_{DP}), the more acidic the alcohol is.

The stabilities of the neutral and anionic (0, $-$) $\text{U} \cdots \text{HOR}$ complexes are expressed in terms of electronic stabilization energy (E_{stab}), E_{stab} corrected for the energy of zero-point vibrations ($E_{stab+ZPVE}$), and free energy of stabilization, G_{stab} . E_{stab} is defined as the difference in electronic energies of the monomers and the dimer

$$E_{stab} = E^{U(0,-)}(\text{geom}^{U(0,-)}) + E^{\text{ROH}}(\text{geom}^{\text{ROH}}) - E^{U(0,-) \cdots \text{HOR}}(\text{geom}^{U(0,-) \cdots \text{HOR}}) \quad (3)$$

with the electronic energy E^X ($X = \text{U}^{(0,-)}, \text{ROH}, \text{U}^{(0,-)} \cdots \text{HOR}$) computed for the coordinates determining the optimal geometry of X (i.e., the geometry where E^X is at the minimum). The values of E_{stab} were not corrected for basis set superposition error,^{58,59} because our earlier results demonstrated that the values of this error in B3LYP/6-31++G** calculations for a similar neutral uracil–glycine complex do not exceed 0.06 eV. Finally, the stabilization Gibbs energy G_{stab} results from supplementing $E_{stab+ZPVE}$ with thermal contributions to energy from vibrations, rotations, and translations, the pV terms, and the entropy term. The values of G_{stab} discussed below were obtained for $T = 298$ K and $p = 1$ atm.

TABLE 2: Evolution of the Structure of the aAnU Complexes as the Gas-Phase Acidity of An Increases

Alcohols	H_{DP} range (eV)	PT?	Example
A1-A8, A10c	16.28 - 14.96, 14.72	No PT on the N3 or C5 side of O8	 aA1UC _U aA1UN _U
A9,A11	14.83, 14.67	Two minima for the N3 side of O8; No PT on the C5 side of O8	 aA9UC _U aA9UN _U aA9UN _{HU}
A10t, A12- A13	14.77, 14.46-14.38	BFPT on the N3 side of O8; No PT on the C5 side of O8	 aA12UC _U aA12UN _{HU}
A14	14.38	BFPT on the N3 side of O8; Two minima on the C5 side of O8	 aA14UC _U aA14UC _{HU} aA14UN _{HU}
A15- A18	14.32 - 13.79	BFPT on the N3 side of O8; BFPT on the C5 side of O8	 aA15UC _{HU} aA15UN _{HU}

All calculations were carried out with the GAUSSIAN 98⁶⁰ and NWChem⁶¹ programs on a PC/Linux cluster, an IBM SP/2, and SGI Origin2000 numerical servers.

III. Alcohols and Complexes

A series of alcohols has been designed with the H_{DP} in the range 16.3–13.8 eV (see Table 1). The enthalpies and free energies of deprotonation of alcohols are usually underestimated at the B3LYP/6-31++G** level, but the discrepancies between the calculated and measured values do not exceed 0.3 eV. From here on, these alcohols will be labeled An ($1 \leq n \leq 18$), and the gas-phase acidity increases as n increases. H₂O is listed in Table 1 as A0 to provide calibration of the calculated values of H_{DP} and for comparison of the (H₂O...U)⁻ complex⁴⁰ with the anionic alcohol–uracil complexes presented here. The most basic alcohol considered by us is ethanol ($H_{DP} = 16.3$ eV), and

the most acidic is CF₃CF₂OH ($H_{DP} = 13.8$ eV). An alcohol A10, 1,1,1,3,3,3-hexafluoro-2-propanol, has two important isomers with different capabilities to form hydrogen bonds with uracil and with different deprotonation enthalpies. These two isomers are shown in Figure 2 and are called A10c (cis form; $H_{DP} = 14.7$ eV) and A10t (trans form; $H_{DP} = 14.8$ eV), with cis and trans referring to the relative positions of the OH and CH hydrogens. The trans isomer is 0.05 eV lower in energy than the cis isomer.

Our earlier results on anionic complexes of uracil with weak acids indicate that the O8 site of uracil is susceptible to intermolecular proton transfer.^{39–41} Moreover, the anionic complexes bound through O8 were more stable than those bound through O7. The favorable properties of the O8 site result from a charge distribution of the excess π^* electron (see Figure 1), which is localized primarily in the O8–C4–C5–C6 region.

Thus, hydrogen bonding through the O8 site stabilizes the anionic complex more strongly than hydrogen bonding through the O7 site. These earlier findings prompted us to restrict the topological space to the structures with a hydrogen bond between the hydroxyl group of an alcohol and the O8 site of uracil. In these structures, the hydroxyl group plays a dual role as both a proton donor and acceptor.

Two such structures are possible with the proton donor of uracil being either the N3H or C5H (see Figures 1 and 3), and the resulting complexes between the A_n alcohol and uracil will be labeled A_nUN and A_nUC , respectively. The A_nUN and A_nUC complexes are analogous to UG14 and UG16, respectively, in the family of uracil–glycine complexes. The anionic UG14 and UG16 complexes were the most stable among those in which an OH group acts as both a proton donor and acceptor.³⁹

The anionic structures characterized in this study will be labeled aX_Y ($X = A_nUC$ or A_nUN , and $Y = U, HU,$ or TS). They are defined as stationary points on the anionic potential energy surface. Two kinds of minima can develop on the anionic potential energy surface: $ROH \cdots U^-$ that describes a hydrogen bond between U^- and an intact alcohol ($Y = U$) and $RO^- \cdots HU$ that develops as a consequence of the proton transfer from the alcohol's OH to O8 of uracil ($Y = HU$). The anionic complexes with BFPT possess only one minimum, that is, aX_{HU} . The anionic complexes without BFPT can have only one (i.e., aX_U) or both minima. In the latter case, there is a transition state that separates the aX_U and aX_{HU} minima, and this stationary point is labeled aX_{TS} . For instance, the symbol $aA3UN_{HU}$ stands for a minimum on the potential energy surface of the anionic complex of uracil with CHF_2CH_2OH , in which uracil is hydrogenated at O8 and RO^- forms another hydrogen bond with N3H of uracil. We will also use a simplified notation when referring to a group of similar complexes. For example, aA_nUC stands for a broad family of anionic complexes with alcohols bonded to the C5 side of O8. Some examples of our notation are shown in Table 2.

IV Results

IV.1. Experimental Data. The photoelectron spectra of anionic complexes of uracil with ethanol, 2,2,3,3,3-pentafluoropropanol, and 1,1,1,3,3,3-hexafluoro-2-propanol, denoted $aA1U$, $aA6U$, and $aA10U$, respectively, are very different (see Figure 4). The main features in the photoelectron spectra of $aA1U$ and $aA6U$ have a maxima at about 1.0 and 1.3 eV, respectively. The spectrum of $aA10U$ is structureless with two broad features: a larger intensity peak at 2.0–2.2 eV and a lower intensity peak at 1.3–1.6 eV.

The valence π^* and dipole-bound anionic states of uracil are characterized by calculated values of the VDE of 0.506 and 0.073 eV, respectively.²⁴ Henceforth, only the valence π^* anionic state will be considered further, since the experimental values of VDE for aA_nU are far too large for the dipole-bound anionic state of U^- solvated by A_n .

The spectra of $aA1U$ and $aA6U$ can be attributed to the valence π^* anionic state of uracil solvated by the corresponding alcohol. Shifts in the VDE from 0.5 eV (U^-) to 1.0 ($aA1U$) and 1.3 ($aA6U$) eV can result from stabilization by the alcohol. A difference in the position of the main feature between $aA1U$ and $aA6U$ can result from different gas-phase acidity of A1 and A6; see Table 1. The interpretation is consistent with our previous results for $U^- \cdots H_2O$ with a measured VDE of 0.9 eV.⁴⁰ Indeed, H_2O with an experimental H_{DP} of 16.9 eV is a weaker acid than ethanol ($H_{DP} = 16.4$ eV); see Table 1.

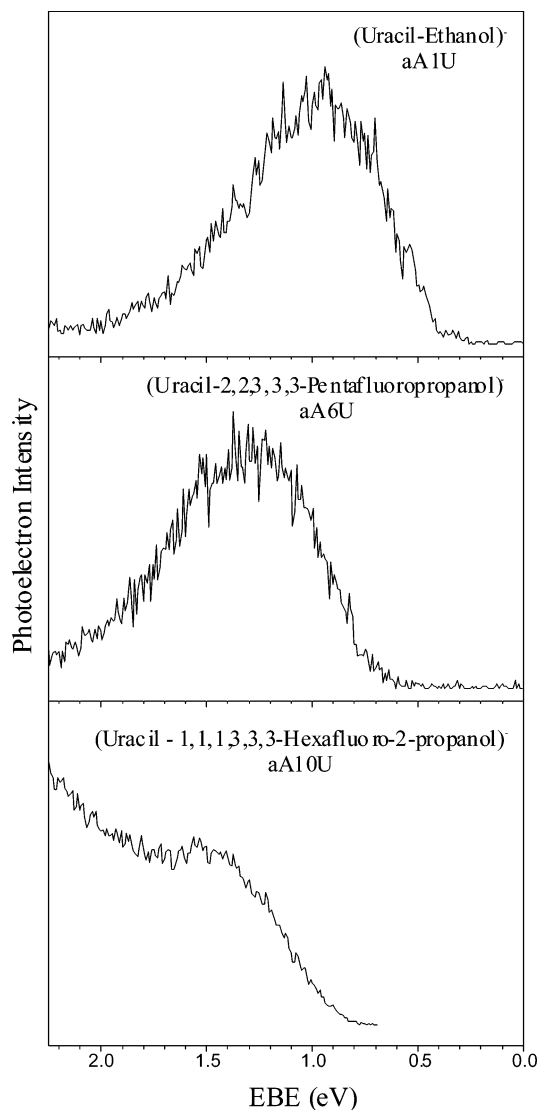


Figure 4. Photoelectron spectra of uracil–alcohol complexes recorded with 2.54 eV photons.

The same interpretation can be applied to a low-energy feature at 1.5–1.7 eV in the photoelectron spectrum of $aA10U$ (see Figure 4), because A10 is more acidic than A6 by ca. 0.5 eV; see Table 1. However, a high-energy feature at 2.0–2.2 eV is difficult to interpret. It might be attributed to U^- in the valence π^* anionic state solvated by A10. The solvation energy of U^- by A10 would have to be larger than that of U^- by A1 by about 1 eV, which is difficult to accomplish. There are, however, cis and trans forms of A10 (see Figure 2), and the CH hydrogen is unusually protic (see Table 1) because of the electron withdrawing effect of two $-CF_3$ groups. The CH hydrogen interacting with the excess electron localized on uracil might contribute to the unusually strong solvation of U^- . Another possible interpretation of a feature at 2.0–2.2 eV is that intermolecular proton transfer develops in some anionic complexes of A10 with uracil, in analogy to the systems studied by us in the past.^{39–41} A proton transfer to the ring of uracil would stabilize the unpaired electron and would result in a substantial increase in the value of VDE. In view of the efficient cooling of nascent anions, it is unlikely that proton transfer is occurring in vibrationally excited anions.

We should comment on the possibility of dissociative electron attachment in our experiments, which has recently been studied for nucleic acid bases in the groups of Illenberger and Mark.^{62,63} We too often see dissociative electron attachment to free U to

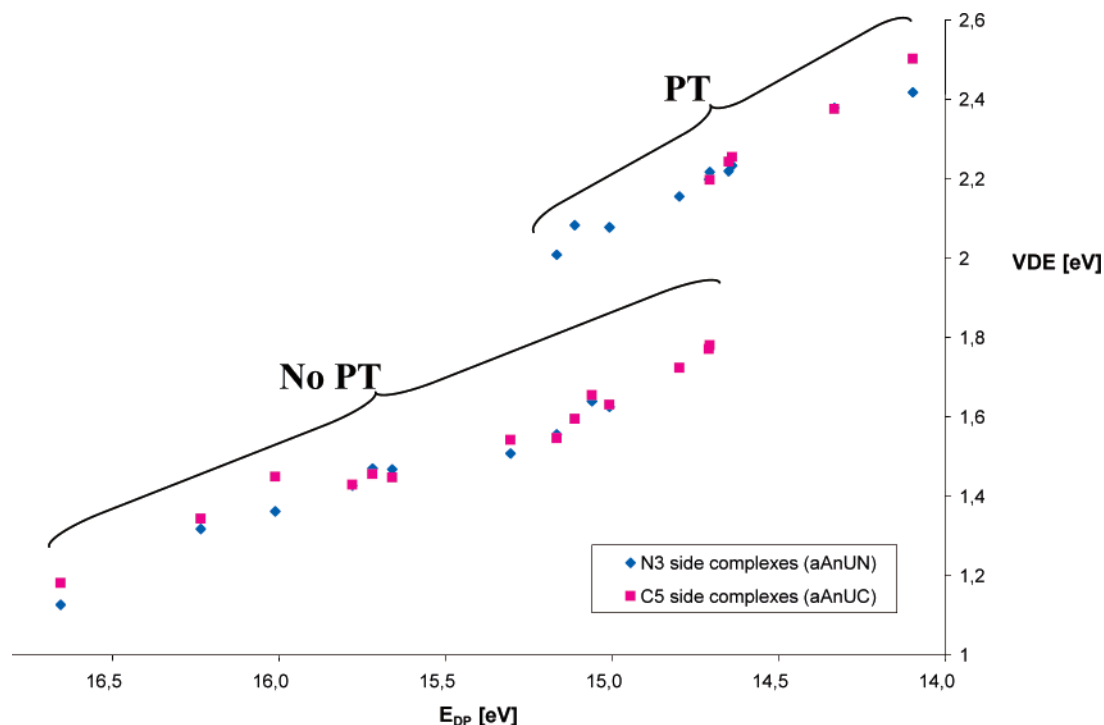


Figure 5. The VDE in anionic uracil–alcohol complexes vs the deprotonation energy (E_{DP}) of the alcohol. All properties calculated at the B3LYP/6-31++G**(5d) level of theory. “PT” and “No PT” are groups of complexes with and without proton transfer, respectively.

yield $(\text{U}-\text{H})^-$, that is, deprotonated uracil. However, in the experiments discussed in this paper, we did not see $(\text{U}-\text{H})^- \cdots \text{HOR}$ complexes in our mass spectra.

IV.2. Computational Results. Quantum chemical calculations were performed for twelve neutral and anionic complexes between uracil and an alcohol. A common feature of anionic wave functions identified by us for the $aAnU$ complexes is that the unpaired electron is localized on a π^* orbital of uracil, in close resemblance to the valence anionic state of isolated uracil (Figure 1). An isolated uracil molecule has a symmetry plane. However, occupation of the antibonding π^* orbital by an excess electron induces buckling of the ring, because nonplanar structures are characterized by a less severe antibonding interaction. The same kind of a ring distortion takes place in all anionic $aAnU$ complexes.

The structures of the $aAnU$ complexes systematically evolve as the gas-phase acidity of An increases (see Table 2). Our calculations strongly suggest that the complexes of anionic uracil with the most basic alcohols (A1–A8; $15.0 < H_{\text{DP}} < 16.3$ eV) are primarily of the $\text{ROH} \cdots \text{U}^-$ type, that is, there is no intermolecular proton transfer. An exception is the aA7U complex, which decomposes with a release of the CCl_3^- group.

The N3 side of O8 is more susceptible to intermolecular proton transfer than the C5 side. Indeed, for the aA9U and aA11U complexes, a minimum of the $\text{RO}^- \cdots \text{HU}^-$ type develops on the N3 side in addition to the $\text{ROH} \cdots \text{U}^-$ minimum (see Table 2). These minima are separated by low-energy barriers; see the relative energies of transition states in Table S1 (Supporting Information). For A9 and A11 bound to the C5 side of O8, only one structure (i.e., $\text{ROH} \cdots \text{U}^-$) was identified.

As the alcohol’s gas-phase acidity further increases, a barrier disappears on the N3 side of O8, and all $aAnUN$ complexes ($n > 11$) are characterized by only one minimum of the $\text{RO}^- \cdots \text{HU}^-$ type (see Table 2). Using our earlier terminology,^{39–41} we would say that these $aAnUN$ complexes undergo BFPT on the N3 side. On the C5 side of O8, however, there is

still no proton transfer for the aA12UC and aA13UC complexes, which support only one minimum of the $\text{ROH} \cdots \text{U}^-$ type.

It requires an H_{DP} as small as 14.4 eV (A14) to support two minima on the C5 side of O8. For even more acidic alcohols ($n > 14$; $H_{\text{DP}} < 14.4$ eV), the $\text{ROH} \cdots \text{U}^-$ minimum disappears with the $\text{RO}^- \cdots \text{HU}^-$ structure being the only minimum for both sides of O8 (see Table 2).

The unpaired electron is always localized on the ring of uracil. The excess charge, on the other hand, is localized on uracil in the case of $\text{ROH} \cdots \text{U}^-$ complexes and on RO^- in the case of $\text{RO}^- \cdots \text{HU}^-$ complexes. Thus, the $\text{ROH} \cdots \text{U}^-$ and $\text{RO}^- \cdots \text{HU}^-$ complexes differ by a proton transfer from ROH to U^- . This proton transfer can be barrier-free, as in the case of anionic complexes of amino acids with pyrimidine bases,³⁹ or there can be a small barrier, as in anionic complexes of pairs of nucleic-acid bases.⁴¹

The evolution of electron vertical detachment energy in the $aAnU$ complexes as the alcohol’s gas-phase acidity increases is illustrated in Figure 5. The values of VDE are larger for more acidic alcohols, which may be explained by the electrostatic interaction. The unpaired electron localized on uracil is better stabilized the more acidic the proton of the ROH moiety is. There is, however, a remarkable effect of intermolecular proton transfer on the values of VDE. A discontinuity in VDE by ca. 0.5 eV separates complexes with a proton being transferred to the uracil ring (i.e., the $\text{RO}^- \cdots \text{HU}^-$ structures) from the $\text{ROH} \cdots \text{U}^-$ structures.

There is also a systematic increase in the values of E_{stab} as the alcohol’s gas-phase acidity increases; see Figure 6. The distribution of E_{stab} values is particularly broad for these values of E_{DP} for which both the $\text{ROH} \cdots \text{U}^-$ and $\text{RO}^- \cdots \text{HU}^-$ structures might coexist. The alcohol is preferably bound to the C5 side of O8 for the $aAnU$ complexes without intermolecular proton transfer and to the N3 side of O8 for the $aAnU$ complexes with intermolecular proton transfer. This is reflected in the values of E_{stab} presented in Figure 6 and Table S1 (Supporting

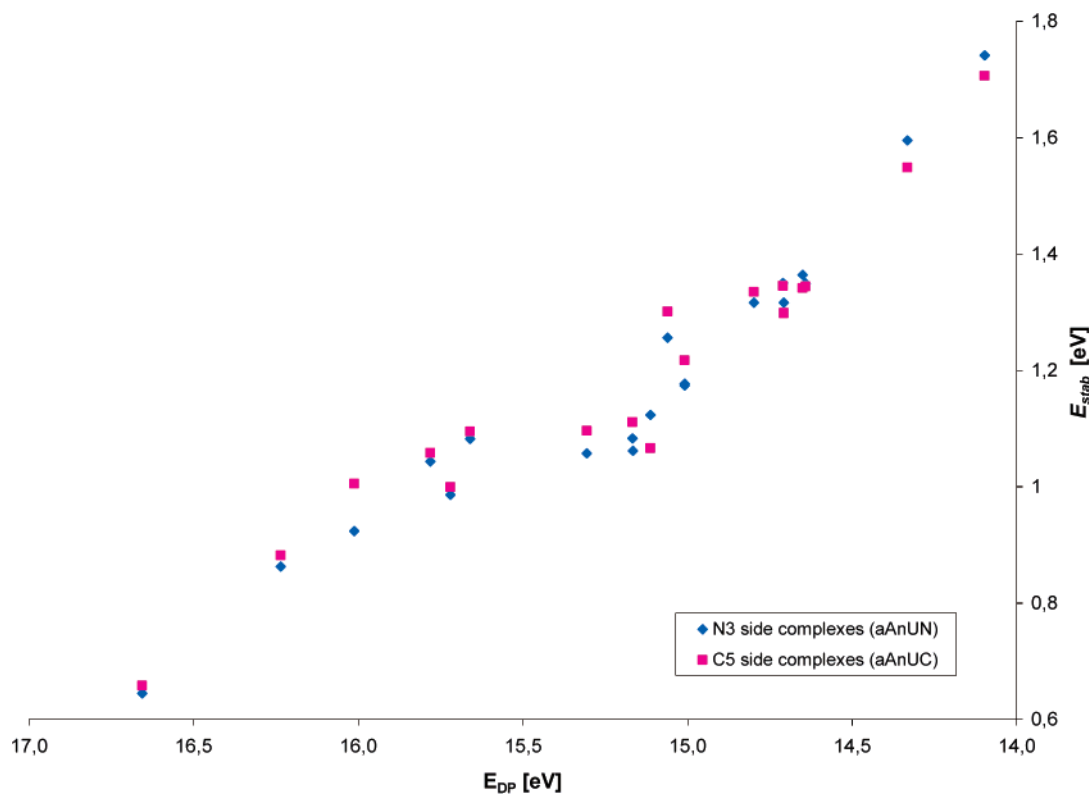


Figure 6. The stabilization energy (E_{stab}) in anionic uracil–alcohol complexes vs the deprotonation energy (E_{DP}) of ROH. All properties calculated at the B3LYP/6-31++G**(5d) level of theory.

Information). This finding is consistent with our result for the $(U \cdots H_2A)^-$ complexes ($A = O, S, Se$).⁴⁰ The anionic complexes *without intermolecular proton transfer* have only one strong hydrogen bond involving the O8 of U and a proton donor site. Then, the C5 side of O8 is a preferable binding direction for the proton donor, because the gas-phase basicity of U^- is larger on the C5 side than the N3 side of O8; see Table 1. The anionic complexes *with intermolecular proton transfer* have an additional hydrogen bond, which involves a deprotonated weak acid (i.e., an anion) and the N3H or the C5H of U. This hydrogen bond is stronger for the former than the latter and provides an additional stabilization reflected in the reported values of E_{stab} .

IV.3. Discussion. The B3LYP values of VDE for the aA1U complex amount to 1.13 and 1.18 eV for the N3 and C5 sides of O8, respectively; see Table S1. When corrected downward by 0.2 eV (a correction based on the CCSD(T) result for U^- ; see section II.2), they approximately overlap with the broad maximum of the PES spectrum of this complex at 1.0 eV; see Figure 4. Similarly, the B3LYP values of VDE for the aA6U complex are 1.45 and 1.47 eV for the C5 and N3 sides of O8, respectively. After the -0.2 eV correction, they approximately overlap with the broad maximum of the PES spectrum of this complex at 1.3 eV.

The aA10U complex can involve either the cis or trans isomers of the A10 alcohol (1,1,1,3,3,3-hexafluoro-2-propanol). The coordination of A10t to the N3 and C5 sides of O8 leads to the $RO^- \cdots HU$ and $ROH \cdots U^-$ minima, respectively, with the former characterized by a VDE value larger by ca. 0.5 eV than the latter. On the other hand, the anionic complexes with A10c do not support the $RO^- \cdots HU$ minima, have similar values of VDE, and are more stable than the complexes involving the more stable isomer, A10t (see Table S1). The four aA10U complexes are presented in Figure 7.

The small differences in the stability of the aA10U complexes and the complexity of the PES spectrum prompted us to perform

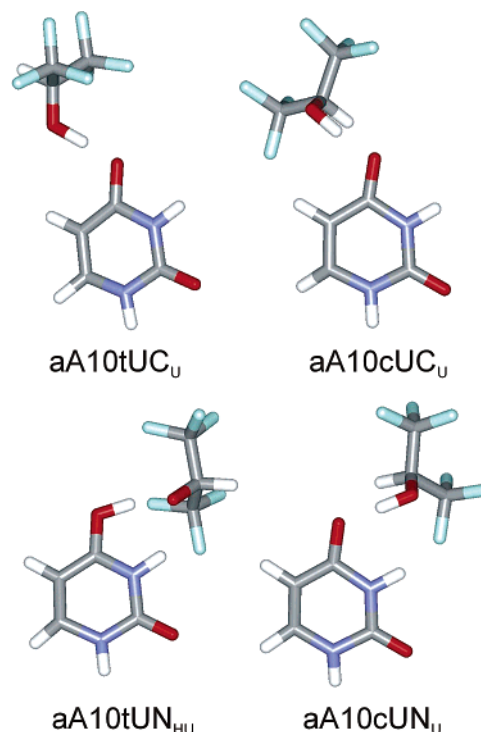


Figure 7. The anionic complexes of uracil with different isomers of A10 (1,1,1,3,3,3-hexafluoro-2-propanol).

MP2 calculations; the resulting relative stabilities of these complexes and the VDE values are presented in Table 3. The MP2 results confirm the occurrence of BFPT for the aA10tUN complex and the lack thereof for the three other complexes. They also confirm that the complexes involving A10c are more stable than the complexes involving A10t. A new and initially unexpected finding is that the MP2 values of VDE for the

TABLE 3: Relative Stability of the aA10U Complexes at the B3LYP and MP2 Levels of Theory and the MP2 Values of VDE^a

complex	ΔE B3LYP	ΔH B3LYP	ΔG B3LYP	ΔE MP2	VDE MP2	VDE _{corr} MP2 ^b
aA10cUC _U	0.000	0.000	0.000	0.000	1.76	1.89
aA10cUN _U	0.045	0.037	0.057	0.048	1.74	1.87
aA10tUN _{HU}	0.128	0.116	0.131	0.147	1.83	1.96
aA10tUC _U	0.185	0.153	0.166	0.207	1.22	1.35

^a All energies in eV obtained with the 6-31++G**(5d) basis set. ^b A +0.13 eV correction applied. The correction is based on the CCSD(T) results for U⁻;²⁴ see section II.2.

complexes with A10c, which do not undergo BFPT, are nearly as large as the VDE value for the aA10tUN complex, which undergoes BFPT. A plausible explanation is that the A10c alcohol can engage both the OH and CH protons in stabilization of the excess charge localized on uracil (see Figure 7). The gas-phase acidity of this CH is comparable to the gas-phase acidity of the A6 alcohol (see Table 1). The structure of A10t, on the other hand, does not facilitate the interaction of CH with U⁻. These factors result in the values of VDE for aA10cUC(N)_U comparable to that of aA10tUN_{HU}, whereas the value of VDE for aA10tUC_U is smaller by ca. 0.5–0.6 eV (see Table 3).

The MP2 values of relative stability and the VDE values for aA10U are consistent with the PES spectrum (see Figure 4). The VDE values for the three most stable structures (aA10cUC_U, aA10cUN_U, and aA10tUN_{HU}) span the range 1.9–2.0 eV and coincide with the position of the more intense feature in the PES spectrum. The VDE value for the least stable aA10tUC_U structure of 1.4 eV coincides with the lower intensity feature in the PES spectrum.

A quantitative interpretation of the PES spectra is hampered by experimental and theoretical uncertainties. First, the relative stabilities of different structures would have to be determined with accuracy much higher than that resulting from current exchange-correlation functionals. Second, in view of significant differences in structure between the neutral and anionic species, the Franck–Condon factors would have to be determined, and anharmonic effects might be important. We should point out that so far we have characterized the ROH \cdots U⁻ and/or RO⁻ \cdots HU \cdot minima on the potential energy surface of the (ROH \cdots U)⁻ complexes. In the case of quasidegenerate ROH \cdots U⁻ and RO⁻ \cdots HU \cdot minima, the description limited to the coexisting classical structures might not be sufficient. In view of the small proton mass, both electrons and the ROH proton should be treated quantum mechanically to include nuclear quantum effects such as zero-point vibration energy and proton tunneling. The multiconfigurational nuclear–electronic orbital method⁶⁴ provides the proper framework to include these effects.

V. Summary

We characterized binary anionic complexes of uracil with alcohols using theoretical and experimental methods. A series of 18 alcohols was designed with the gas-phase enthalpy of deprotonation in the range 13.8–16.3 eV. The photoelectron spectra of anionic complexes of uracil with 3 of these alcohols were measured with 2.54 eV photons. Our main conclusions are as follows:

- For ROHs with deprotonation enthalpies larger than 14.8 eV, only the ROH \cdots U⁻ minimum exists on the potential energy surface. Two minima might coexist on the anionic energy surface for $14.3 < H_{DP} < 14.8$ eV. These minima correspond to the RO⁻ \cdots HU \cdot and ROH \cdots U⁻ structures. For ROHs with H_{DP} smaller than 14.3 eV, an intermolecular barrier-free proton transfer always takes place with the product being RO⁻ \cdots HU \cdot . The N3 side of O8 is more susceptible to intermolecular proton transfer than the C5 side.

- The values of electron vertical detachment energy systematically increase as the gas-phase acidity of the alcohol increases. There is, however, a discontinuity in VDE by ca. 0.5 eV, which is a manifestation of intermolecular proton transfer.

- The stabilization energy of anionic complexes systematically increases as the gas-phase acidity of the alcohol increases. The alcohol is preferably bound to the C5 side of O8 for the aAnU complexes without intermolecular proton transfer and to the N3 side of O8 for the aAnU complexes with intermolecular proton transfer.

- The measured photoelectron spectra for anionic complexes of uracil with ethanol, 2,2,3,3,3-pentafluoropropanol, and 1,1,1,3,3,3-hexafluoro-2-propanol are in qualitative agreement with computational results. We assign the ROH \cdots U⁻ structure to the first two complexes. A difference in the position of the main PES feature can result from a different gas-phase acidity of ethanol and 2,2,3,3,3-pentafluoropropanol.

- The spectrum of the anionic complex of uracil with 1,1,1,3,3,3-hexafluoro-2-propanol (A10) displays two broad features: a larger intensity peak at 2.0–2.2 eV and a lower intensity feature at 1.5–1.7 eV. This spectrum was interpreted in terms of anionic complexes of U with the cis and trans isomers of A10. Only the latter coordinated to the N3 side of O8 undergoes BFPT.

Acknowledgment. This work was supported by the Polish State Committee for Scientific Research (KBN) grant 4T09A01224 (J.R. and M.H.), the National Science Foundation (NSF) grant CHE 0211522 (K.B.), and the U.S. DOE, Office of Biological and Environmental Research, Office of Science, Low Dose Radiation Research Program (M.G.). Computing resources have been available through (i) Computational Grand Challenge Application grant from the Molecular Sciences Computing Facility (MSCF) in the Environmental Molecular Sciences Laboratory, (ii) the National Energy Research Scientific Computing Center (NERSC), and (iii) the Academic Computer Center in Gdańsk (TASK). The MSCF is funded by DOE's Office of Biological and Environmental Research. PNNL is operated by Battelle for the U.S. DOE under contract DE-AC06-76RLO 1830.

Supporting Information Available: Energy of stabilization and electron vertical detachment energy (VDE) for the anionic uracil–alcohol complexes bonded through O8 of uracil. This material is available free of charge via the Internet at <http://pubs.acs.org>.

References and Notes

- (1) Steenken, S. *Chem. Rev.* **1989**, *89*, 503–520.
- (2) Boudaiffa, B.; Cloutier, P.; Hunting, D.; Huels, M. A.; Sanche, L. *Science* **2000**, *287*, 1658–1660.
- (3) Green, N. J. B.; Bolton, C. E.; Spencer-Smith, R. D. *Radiat. Environ. Biophys.* **1999**, *38*, 221–228.
- (4) Desfrancois, C.; Carles, S.; Schermann, J. P. *Chem. Rev.* **2000**, *100*, 3943–3962.
- (5) Oylar, N. A.; Adamowicz, L. *J. Phys. Chem.* **1993**, *97*, 11122–11123.

- (6) Smets, J.; McCarthy, W. J.; Adamowicz, L. *J. Phys. Chem.* **1996**, *100*, 14655–14660.
- (7) Smets, J.; Smith, D. M. A.; Elkadi, Y.; Adamowicz, L. *J. Phys. Chem. A* **1997**, *101*, 9152–9156.
- (8) Dolgounitcheva, O.; Zakrzewski, V. G.; Ortiz, J. V. *Chem. Phys. Lett.* **1999**, *307*, 220–226.
- (9) Dolgounitcheva, O.; Zakrzewski, V. G.; Ortiz, J. V. *J. Phys. Chem. A* **1999**, *103*, 7912–7917.
- (10) Gutowski, M.; Skurski, P.; Simons, J. *J. Am. Chem. Soc.* **2000**, *122*, 10159–10162.
- (11) Skurski, P.; Rak, J.; Simons, J.; Gutowski, M. *J. Am. Chem. Soc.* **2001**, *123*, 11073–11074.
- (12) Rak, J.; Skurski, P.; Gutowski, M. *J. Chem. Phys.* **2001**, *114*, 10673–10681.
- (13) Wesolowski, S. S.; Leininger, M. L.; Pentchev, P. N.; Schaefer, H. F., III. *J. Am. Chem. Soc.* **2001**, *123*, 4023–4028.
- (14) Hendricks, J. H.; Lyapustina, S. A.; de Clercq, H. L.; Snodgrass, J. T.; Bowen, K. H. *J. Chem. Phys.* **1996**, *104*, 7788–7791.
- (15) Hendricks, J. H.; Lyapustina, S. A.; de Clercq, H. L.; Bowen, K. H. *J. Chem. Phys.* **1998**, *108*, 8–11.
- (16) Schiedt, J.; Weinkauff, R.; Neumark, D. M.; Schlag, E. W. *Chem. Phys.* **1998**, *239*, 511–524.
- (17) Desfrancois, C.; Abdoul-Carime, H.; Schermann, J. P. *J. Chem. Phys.* **1996**, *104*, 7792–7794.
- (18) Desfrancois, C.; Periquet, V.; Bouteiller, Y.; Schermann, J. P. *J. Phys. Chem. A* **1998**, *102*, 1274–1278.
- (19) Sevilla, M. D.; Besler, B.; Colson, A. O. *J. Phys. Chem.* **1994**, *98*, 2215–2215.
- (20) Sevilla, M. D.; Besler, B.; Colson, A. O. *J. Phys. Chem.* **1995**, *99*, 1060–1063.
- (21) Li, X.; Cai, Z.; Sevilla, M. D. *J. Phys. Chem. A* **2002**, *106*, 1596–1603.
- (22) Harańczyk, M.; Gutowski, M. *J. Am. Chem. Soc.* **2005**, *127*, 699–706.
- (23) Harańczyk, M.; Rak, J.; Gutowski, M. *J. Am. Chem. Soc.* Submitted for publication.
- (24) Bachorz, R. A.; Rak, J.; Gutowski, M. *Phys. Chem. Chem. Phys.* **2005**, *7*, 2116.
- (25) Aflatooni, K.; Gallup, G. A.; Burrow, P. D. *J. Phys. Chem. A* **1998**, *102*, 6205–6207.
- (26) Lowdin, P. O. *Rev. Mod. Phys.* **1963**, *35*, 724–732.
- (27) Estrin, D. A.; Paglieri, L.; Corongiu, G. *J. Phys. Chem.* **1994**, *98*, 5653–5660.
- (28) Morpugo, S.; Bossa, M.; Morpugo, G. O. *Chem. Phys. Lett.* **1997**, *280*, 233–238.
- (29) Kryachko, E. S.; Nguyen, M. T.; Zeegers-Huyskens, T. *J. Phys. Chem. A* **2001**, *105*, 1288–1295.
- (30) Kryachko, E. S.; Nguyen, M. T.; Zeegers-Huyskens, T. *J. Phys. Chem. A* **2001**, *105*, 1934–1943.
- (31) Hobza, P.; Sponer, J. *Chem. Rev.* **1999**, *99*, 3247–3276.
- (32) Kim, Y.; Lim, S.; Kim, Y. *J. Phys. Chem. A* **1999**, *103*, 6632–6637.
- (33) Bertran, J.; Olivia, A.; Rodriguez-Santiago, L.; Sodupe, M. *J. Am. Chem. Soc.* **1998**, *120*, 8159–8167.
- (34) Takeuchi, S.; Tahara, T. *Chem. Phys. Lett.* **1997**, *277*, 340–346.
- (35) Zhanpeisov, N. U.; Sponer, J.; Leszczynski, J. *J. Phys. Chem. A* **1998**, *102*, 10374–10379.
- (36) He, F.; Ramirez, J.; Lebrilla, C. B. *J. Am. Chem. Soc.* **1999**, *121*, 4726–4727.
- (37) Li, X.; Cai, Z.; Sevilla, M. D. *J. Phys. Chem. A* **2001**, *105*, 10115–10123.
- (38) Dąbkowska, I.; Rak, J.; Gutowski, M. Submitted for publication.
- (39) Gutowski, M.; Dąbkowska, I.; Rak, J.; Xu, S.; Nilles, J. M.; Radisic, D.; Bowen, K. H., Jr. *Eur. Phys. J. D* **2002**, *20*, 431–439.
- (40) Harańczyk, M.; Bachorz, R.; Rak, J.; Gutowski, M.; Radisic, D.; Stokes, S. T.; Nilles, J. M.; Bowen, K. H. *J. Phys. Chem. B* **2003**, *107*, 7889–7895.
- (41) Radisic, D.; Bowen, K. H., Jr.; Dąbkowska, I.; Stononiak, P.; Rak, J.; Gutowski, M. *J. Am. Chem. Soc.* **2005**, *127*, 6443–6450.
- (42) Coe, J. V.; Snodgrass, J. T.; Freidhoff, C. B.; McHugh, K. M.; Bowen, K. H. *J. Chem. Phys.* **1987**, *87*, 4302–4309.
- (43) Coe, J. V.; Snodgrass, J. T.; Freidhoff, C. B.; McHugh, K. M.; Bowen, K. H. *J. Chem. Phys.* **1986**, *84*, 618–625.
- (44) Becke, A. D. *Phys. Rev. A* **1988**, *38*, 3098–3100.
- (45) Becke, A. D. *J. Chem. Phys.* **1993**, *98*, 5648–5652.
- (46) Lee, C.; Yang, W.; Parr, R. G. *Phys. Rev. B* **1988**, *37*, 785–789.
- (47) Ditchfield, R.; Hehre, W. J.; Pople, J. A. *J. Chem. Phys.* **1971**, *54*, 724–728.
- (48) Hehre, W. J.; Ditchfield, R.; Pople, J. A. *J. Chem. Phys.* **1972**, *56*, 2257–2261.
- (49) Dąbkowska, I.; Rak, J.; Gutowski, M. *J. Phys. Chem. A* **2002**, *106*, 7423–7433.
- (50) Rak, J.; Skurski, P.; Simons, J.; Gutowski, M. *J. Am. Chem. Soc.* **2001**, *123*, 11695–11707.
- (51) van Mourik, T.; Price, S. L.; Clary, D. C. *J. Phys. Chem. A* **1999**, *103*, 1611–1618.
- (52) Dkhissi, A.; Adamowicz, L.; Maes, G. *J. Phys. Chem. A* **2000**, *104*, 2112–2119.
- (53) Rienstra-Kiracofe, J. C.; Tschumper, G. S.; Schaefer, H. F., III. *Chem. Rev.* **2002**, *102*, 231–282.
- (54) Simons, J.; Jordan, K. D. *Chem. Rev.* **1987**, *87*, 7, 535–555.
- (55) Gutowski, M.; Simons, J. *J. Chem. Phys.* **1990**, *93*, 2546–2553.
- (56) Modelli, A. *Phys. Chem. Chem. Phys.* **2003**, *5*, 2923–2930.
- (57) Mariano, D.; Vera, A.; Pierini, A. B. *Phys. Chem. Chem. Phys.* **2004**, *6*, 2899–2903.
- (58) Gutowski, M.; Chalasinski, G. *J. Chem. Phys.* **1993**, *98*, 5540–5554.
- (59) Gutowski, M.; van Duijneveldt-van de Rijdt, J.; van Lenthe, J. H.; van Duijneveldt, F. B. *J. Chem. Phys.* **1993**, *98*, 4728–4737.
- (60) Frisch, M. J.; Trucks, G. W.; Schlegel, H. B.; Scuseria, G. E.; Robb, M. A.; Cheeseman, J. R.; Zakrzewski, V. G.; Montgomery, J. A., Jr.; Stratmann, R. E.; Burant, J. C.; Dapprich, S.; Millam, J. M.; Daniels, A. D.; Kudin, K. N.; Strain, M. C.; Farkas, O.; Tomasi, J.; Barone, V.; Cossi, M.; Cammi, R.; Mennucci, B.; Pomelli, C.; Adamo, C.; Clifford, S.; Ochterski, J.; Petersson, G. A.; Ayala, P. Y.; Cui, Q.; Morokuma, K.; Malick, D. K.; Rabuck, A. D.; Raghavachari, K.; Foresman, J. B.; Cioslowski, J.; Ortiz, J. V.; Stefanov, B. B.; Liu, G.; Liashenko, A.; Piskorz, P.; Komaromi, I.; Gomperts, R.; Martin, R. L.; Fox, D. J.; Keith, T.; Al-Laham, M. A.; Peng, C. Y.; Nanayakkara, A.; Gonzalez, C.; Challacombe, M.; Gill, P. M. W.; Johnson, B. G.; Chen, W.; Wong, M. W.; Andres, J. L.; Head-Gordon, M.; Replogle, E. S.; Pople, J. A. *Gaussian 98*; Gaussian, Inc.: Pittsburgh, PA, 1998.
- (61) Straatsma, T. P.; Aprà, E.; Windus, T. L.; Bylaska, E. J.; de Jong, W.; Hirata, S.; Valiev, M.; Hackler, M.; Pollack, L.; Harrison, R.; Dupuis, M.; Smith, D. M. A.; Nieplocha, J.; Tipparaju V.; Krishnan, M.; Auer, A. A.; Brown, E.; Cisneros, G.; Fann, G.; Früchtl, H.; Garza, J.; Hirao, K.; Kendall, R.; Nichols, J.; Tsemekhman, K.; Wolinski, K.; Anshell, J.; Bernholdt, D.; Borowski, P.; Clark, T.; Clerc, D.; Dachsels, H.; Deegan, M.; Dyall, K.; Elwood, D.; Glendening, E.; Gutowski, M.; Hess, A.; Jaffe, J.; Johnson, B.; Ju, J.; Kobayashi, R.; Kutteh, R.; Lin, Z.; Littlefield, R.; Long, X.; Meng, B.; Nakajima, T.; Niu, S.; Rosing, M.; Sandrone, G.; Stave, M.; Taylor, H.; Thomas, G.; van Lenthe, J.; Wong, A.; Zhang, Z.; *NWChem, A Computational Chemistry Package for Parallel Computers, Version 4.6* (2004), Pacific Northwest National Laboratory, Richland, Washington 99352-0999, USA.
- (62) Hanel, G.; Gstir, B.; Denifl, S.; Scheier, P.; Probst, M.; Farizon, B.; Farizon, M.; Illenberger, E.; Mark, T. D. *Phys. Rev. Lett.* **2003**, *90*, 188105.
- (63) Abdoul-Carime, H.; Gohlke, S.; Illenberger, E. *Phys. Rev. Lett.* **2004**, *92*, 168103.
- (64) Webb, S.; Iordanov, T.; Hammes-Schiffer, S. *J. Chem. Phys.* **2002**, *117*, 4106–4118.
- (65) Smith, J. R.; Kim, J. B.; Lineberger, W. C. *Phys. Rev. A* **1997**, *55*, 2036–2043.
- (66) Ramond, T. M.; Davico, G. E.; Schwartz, R. L.; Lineberger, W. C. *J. Chem. Phys.* **2000**, *112*, 1158–1169.
- (67) Graul, S. T.; Schnute, M. E.; Squires, R. R. *Int. J. Mass Spectrom. Ion Processes* **1990**, *96*, 181–198.
- (68) Bartmess, J. E.; Scott, J. A.; McIver, R. T., Jr. *J. Am. Chem. Soc.* **1979**, *101*, 6046–6056.
- (69) Dawson, J. H. J.; Jennings, K. R. *Int. J. Mass Spectrom. Ion Phys.* **1977**, *25*, 47–53.
- (70) Taft, R. W.; Koppel, I. J.; Topsom, R. D.; Anvia, F. *J. Am. Chem. Soc.* **1990**, *112*, 2047–2052.